Tuning of Thermochromic Properties of Polydiacetylene toward Universal Temperature Sensing Materials through Amido Hydrogen Bonding

ARTICLE *in* MACROMOLECULES · JANUARY 2010

Impact Factor: 5.8 · DOI: 10.1021/ma902282c

7 AUTHORS, INCLUDING:

Sumrit Wacharasindhu
Chulalongkorn University
43 PUBLICATIONS **713** CITATIONS
SEE PROFILE

Gamolwan Tumcharern
National Nanotechnology Center, Thailand
51 PUBLICATIONS **642** CITATIONS
SEE PROFILE

Mongkol Sukwattanasinitt
Chulalongkorn University
89 PUBLICATIONS **1,010** CITATIONS
SEE PROFILE

716 *Macromolecules* **2010**, *43*, 716–724
DOI: 10.1021/ma902282c

Macromolecules
ARTICLE

Tuning of Thermochromic Properties of Polydiacetylene toward Universal Temperature Sensing Materials through Amido Hydrogen Bonding

Sumrit Wacharasindhu,[†] Suriyakamon Montha,[‡] Jasuma Boonyiseng,[‡] Anupat Potisatityuenyong,[†] Chaiwat Phollookin,[†] Gamolwan Tumcharern,[§] and Mongkol Sukwattanasinitt*,[†]

[†]*Organic Synthesis Research Unit, Department of Chemistry, Faculty of Science, Chulalongkorn University, Bangkok 10330, Thailand,* [‡]*Program of Petrochemistry and Polymer Science, Faculty of Science, Chulalongkorn University, Bangkok, Thailand, and* [§]*Thailand National Nanotechnology Center, National Science and Technology Development Agency, Patumthanee 12120, Thailand*

Received October 18, 2009; Revised Manuscript Received December 9, 2009

ABSTRACT: Mono- and diamides derivatives of 10,12-pentacosadiynoic acid (PCDA) were synthesized from condensation of PCDA with various aliphatic and aromatic diamines. Polydiacetylenes of the amido-PCDA derivatives were prepared by photopolymerization of their molecular assembly homogeneously dispersed in aqueous media. Thermochromic properties of the resulting polydiacetylene sol were studied by temperature variable UV−vis spectrometry along with photographic recording. The color transition temperatures and thermochromic reversibility of the polymers are varied depended on the number of amide groups and the structure of the aliphatic and aromatic linkers. The phenylenediamide and polymethylenediamide PCDA derivatives give polydiacetylenes with complete thermochromic reversibility, while the polydiacetylenes obtained from 1,2-cyclohexylene and glycolic chain diamide derivatives exhibited irreversible thermochromism, whereas the polymers attained from the aromatic monoamide analogues are partially reversible. The variation of the linkers also allows the color transition temperature of the polydiacetylene to be tuned in the range of 20 °C to over 90 °C. The results provide a fundamental idea about the factors affecting the thermochromic properties of polydiacetylenes toward the development of materials for universal thermal indicators.

Introduction

Although temperature is one of the most important physical parameters affecting quality of various products such as foods, beverages, medicines, and chemicals, temperature indicators for these products are rarely spotted due largely to the lack of economical and biologically safe materials suitable for sensing and displaying the temperature of different types of products. Mercury, the earliest and most widely used temperature sensing material, is too toxic to be safely fabricated on any consumer products. The more recently developed temperature sensing materials such as small molecule liquid crystals and leuco dyes are so precarious that they generally require additional encapsulation for improved stability and safety. Because of their polymeric nature and distinct thermochromic color transition, polydiacetylenes (PDAs) stand a good chance to be developed into economical and safe universal temperature indicators.

The preparation of PDAs was initially achievable via solid-state polymerization of certain diacetylene compounds in their crystalline forms.[1] Later, amphiphilic diacetylenes were found to be polymerized in forms of lipid monolayer and bilayer assemblies.[2] This type of amphiphilic diacetylene has recently emerged as one of the most studied class of diacetylene monomers as they can also form various nanostructures such as vesicles, tubes, and ribbons.[3] The formation of nanovesicles allows the diacetylenes to be dispersed in aqueous media which can be polymerized efficiently by UV-irradiation to produce homogeneous sol of PDA vesicles that spur immense interests in the field of chemical[4] and biological[5] sensors. One of the most commonly used amphiphilic monomers for preparation of vesicles is 10,12-pentacosadiynoic acid (PCDA) lipid which gives an intense blue sol of poly(PCDA) upon photopolymerization. Poly(PCDA) vesicle sol shows irreversible color transition from blue to red upon increasing temperature, pH, or lipophilicity.[6]

Thermochromism is one of the earliest reported chromic properties of polydiacetylene[7] that its mechanism and applications have become subjects of interest in the field of organic materials.[8] The availability of methods for preparation of homogeneous sol of PDA vesicles and new structural relevance of PDA thermochromism have recently been reported. Polydiacetylene vesicles which composed of different position of diacetylene functional group and chain length gave variable colorimetric responses to temperature.[9] Hydrogen bonding between the carboxylic acid headgroups and the interactions between aromatic moiety in lipid assemblies have been proven to be essential for the reversibility of thermochromism of PDAs.[10] These investigations have provided important information for systematic development of PDAs with tunable thermochromic properties. In this contribution, we would like to report synthesis and study of another class of diacetylene lipids which contain one or two hydrogen bond forming amide headgroups. The amide functional group not only can form strong hydrogen bond comparable to the carboxylic group but also can be attached to a substituent without losing all its hydrogen bond forming ability. We synthesized diacetylene lipids containing either one or two amide moieties from the condensation of PCDA with various diamine compounds. The studies on thermochromism of PDAs synthesized in this work allow us to grade the thermochromic

*Corresponding author. E-mail smongkol@chula.ac.th.

 Published on Web 12/29/2009

Scheme 1. Synthesis of Diacetylene Lipid Monomers

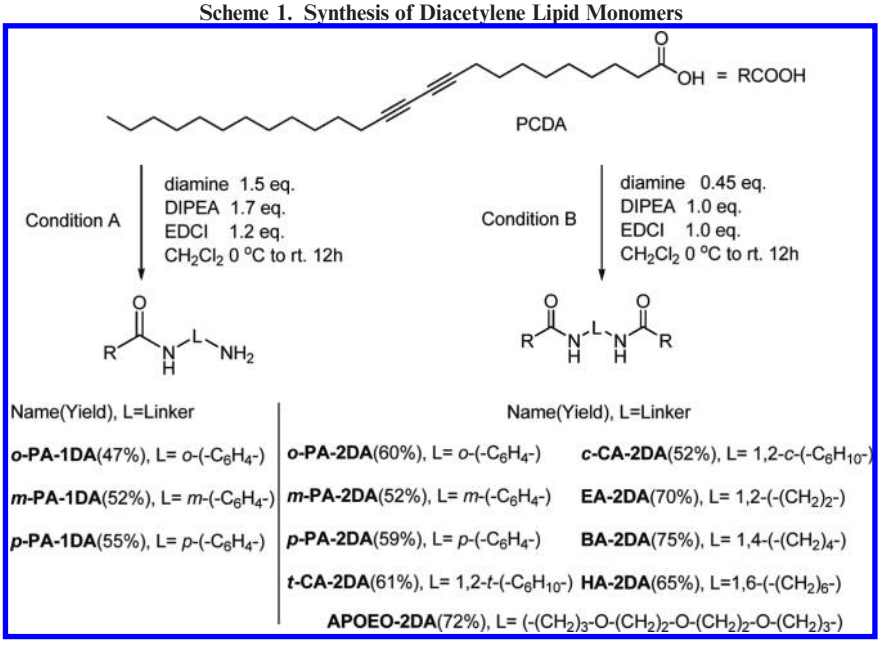

reversibility and tune the color transition temperature to provide structural design and increase the assortment of PDA-based universal temperature sensing materials.

Results and Discussion

Preparation of Diacetylene Monomers. The diacetylene lipid monomers were synthesized via condensation of commercially available PCDA with an appropriate diamine shown in Scheme 1. In condition A, PCDA was reacted with 1.5 equiv of the diamine, i.e., 1,2-phenylenediamine, 1,3-phenylenediamine, and 1,4-phenylenediamine, in the presence of 1-ethyl-3-(3′-dimethylamino)carbodiimide HCl salt (EDCI) as a coupling reagent to afford monoamidodiacetylene. *N*-(2-Aminophenyl)pentacosa-10,12-diynamide (*o*-PA-1DA), *N*-(3-aminophenyl)pentacosa-10,12-diynamide (*m*-PA-1DA), and *N*-(4-aminophenyl)pentacosa-10,12-diynamide (*p*-PA-1DA) were isolated as a white solid in low to moderate yield (29−61%). Low isolated yield was partially caused by the formation of the diamido compounds (ca. 10%) which had to be separated from the monoamido products by column chromatography. In the synthesis of diamidodiacetylenes (condition B), 2 equiv of PCDA was reacted with the diamines to afford the desired product: *N,N*′-(1,2-phenylene)dipentacosa-10,12-diynamide (*o*-PA-2DA), *N,N*′-(1,3-phenylene)dipentacosa-10,12-diynamide (*m*-PA-2DA), and *N,N*′-(1,4-phenylene)dipentacosa-10,12-diynamide (*p*-PA-2DA) in moderate yield (52−60%). The products were conveniently purified by recrystallization in MeOH. Besides phenylenediamine, 1,2-ethylenediamine, 1,4-butylenediamine, 1,6-hexylenediamine, 1,2-*cis*-diaminocyclohexane, *rac*-1,2-*trans*-diaminocyclohexane, and bis((3-aminopropyloxy)ethylene)oxide were also used to react with 2 equiv of PCDA to generate EA-2DA, BA-2DA, HA-2DA, *c*-CA-2DA, *t*-CA-2DA, and APOEO-2DA in moderate to good yields (52−75%).

Preparation of Polydiacetylene Sols. The synthesized monomers were transformed into aqueous polydiacetylene (PDA) sols by sonication of lipid monomer in Milli-Q water followed by irradiation with UV light. The ability to be hydrated and the color of polymerized diacetylenes are presented in Table 1. All monoamide monomers, *o*-PA-1DA, *m*-PA-1DA, and *p*-PA-1DA, could be hydrated to give colorless sol upon sonication at 70−80 °C. On the other hand, diamidodiacetylene such as *o*-PA-2DA, *m*-PA-2DA, *p*-PA-2DA, *t*-CA-2DA, *c*-CA-2DA, BA-2DA, HA-2DA, and APOEO-2DA gave poor dispersion after normal sonication condition due to their high melting temperature (90−128 °C). The dispersion can be improved by repeating the heating and the sonicating process until the translucent sols are obtained. Upon subsequent irradiation of the dispersed monomers with UV light, the colorless sols of *o*-PA-1DA, *m*-PA-1DA, and *p*-PA-1DA readily turned to distinct blue sols, signifying the polymerization of diacetylene

Table 1. Hydration Property of the DA Lipids upon Sonication in Water, Color Appearance, and the Maximum Absorption Wavelength (λ_{max}) of the DA Sols after UV Irradiation

Diacetylene	Linker	Hydratability*	Color (λ_{max}, nm)
PCDA	-	Good	(631, 580)
o-PA-1DA	*o*-(-C_6H_4-)	Good	(631, 580)
m-PA-1DA	*m*-(-C_6H_4-)	Fair	(623, 578)
p-PA-1DA	*p*-(-C_6H_4-)	Fair	(629, 579)
o-PA-2DA	*o*-(-C_6H_4-)	Poor	NA
m-PA-2DA	*m*-(-C_6H_4-)	Fair	(641, 590)
p-PA-2DA	*p*-(-C_6H_4-)	Good	(633, 582)
t-CA-2DA	1,2-*t*-(-C_6H_{10}-)	Good	(640, 588)
c-CA-2DA	1,2-*c*-(-C_6H_{10}-)	Fair	(629, 564)
EA-2DA	1,2-(-$(CH_2)_2$-)	Good	(636, 585)
BA-2DA	1,4-(-$(CH_2)_4$-)	Good	(675, 620, 575)
HA-2DA	1,6-(-$(CH_2)_6$-)	Good	(677, 623, 576)
APOEO-2DA	(-$(CH_2)_3$-O-(CH_2)-)$_2$-O-	Fair	(633, 582)

* Good = translucent sol obtained, fair = semitranslucent sol obtained, poor = no dispersion.

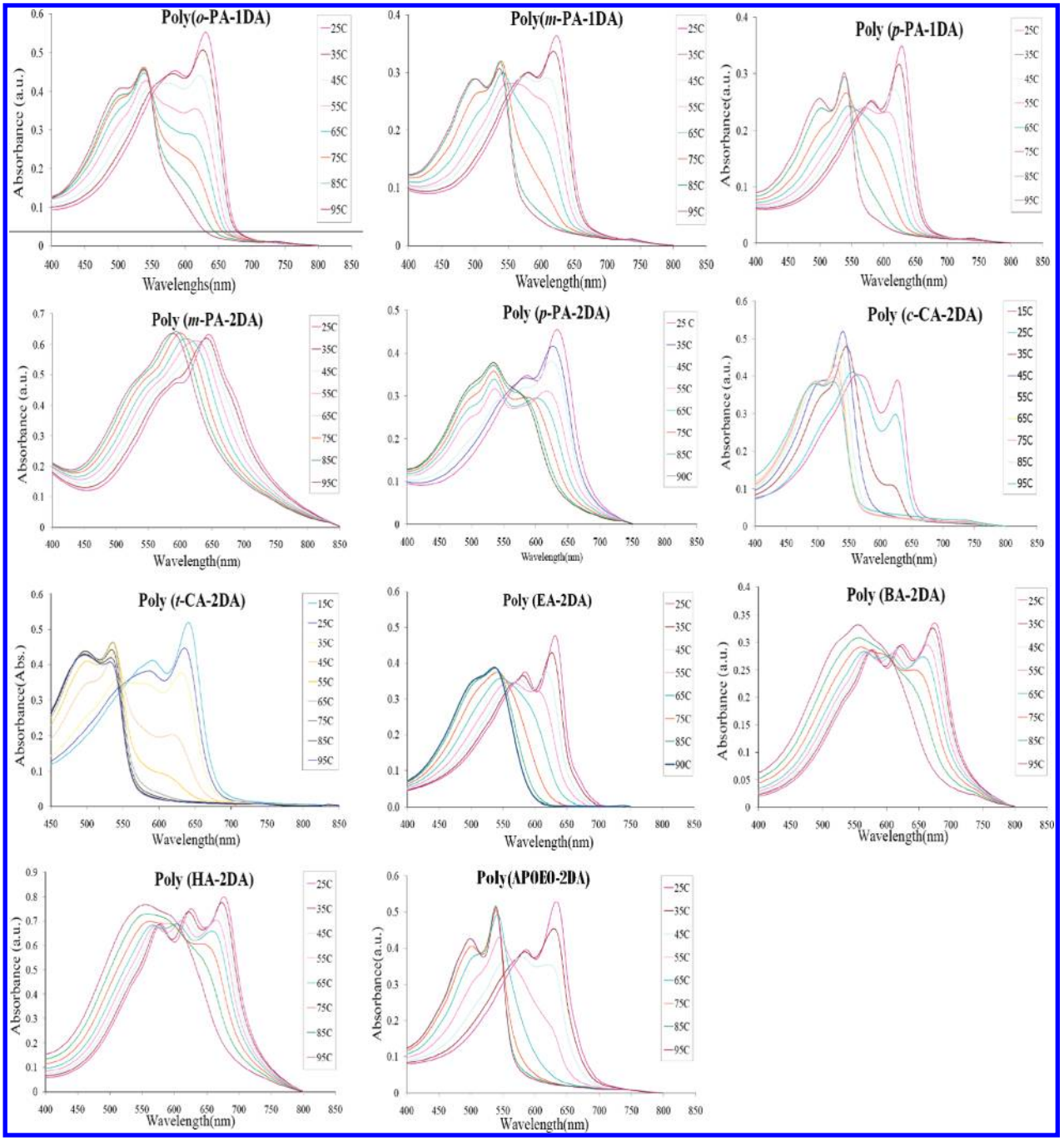

Figure 1. Electronic absorption spectra of PDA sols recorded during stepwise heating.

monomers to form ene−yne conjugated PDAs. The results also support the formation of ordered diacetylene monomer assembly before the polymerization step. The sols of poly(*o*-PA-1DA), poly(*m*-PA-1DA), and poly(*p*-PA-1DA) showed the maximum absorption wavelength (λ_{max}) near 630 nm along with the phonon sideband around 580 nm. The similar blue sols were also obtained from the irradiation of *m*-PA-2DA and *p*-PA-2DA sols. Nevertheless, *o*-PA-2DA rapidly formed blue aggregates upon irradiation. This observation is probably associated with the intramolecular hydrogen bonding between N−H and C═O moieties at the *ortho*-position, reducing the stability of the colloidal particles.

For *t*-CA-2DA and *c*-CA-2DA, reddish-purple sols with λ_{max} below 600 nm were obtained upon exposure to UV at room temperature. The results suggest that the nonplanar dihedral angle between the 1,2-cyclohexylene bonds, connecting to the amide groups, in the diequatorial *trans*-isomer and the axial−equatorial *cis*-isomer do not allow proper packing between the diactylene chains. In an attempt to generate the blue sols of poly(*t*-CA-2DA) and poly(*c*-CA-2DA), the irradiation was conducted in an ice bath (∼5 °C) to reduce the bond vibration. A clear blue sol was produced in the case of *t*-CA-2DA while a purple sol was obtained from *c*-CA-2DA, implying a slightly poorer chain packing of *c*-CA-2DA compared to *t*-CA-2DA. In addition, the colorless sol of EA-2DA having ethylene chain as a linker rapidly turned blue ($\lambda_{max} \sim 636$ nm) upon exposure to UV irradiation at room temperature. Interestingly, with longer linkers like butylene and hexylene, PDA sols prepared from BA-2DA and HA-2DA showed a new absorption maximum at curiously longer wavelength of over 675 nm, along with the

usual absorption bands around 620 and 575 nm. The three absorption peaks including the one at 675 nm observed here is quite different from the recently reported observation of long wavelength absorption caused by the crystal size effect.[11] It is also important to note here that, with the same starting concentration of the monomeric lipids, the polymers obtained from BA-2DA and HA-2DA show the deepest blue color. The low-energy absorption and the highly intense blue color suggest either unusually high backbone strain or long conjugation length associated with superior packing of the long aliphatic linkers between the amide groups. The low-energy absorption band was not observed when the aliphatic alkyl chain linker was replaced with a glycolic chain as in poly(APOEO-2DA) of which only the typical λ_{max} of 633 and 582 nm were observed.

The dynamic light scattering (DLS) was performed to determine the particle size distribution of selected PDA sols. The average particle sizes of poly(*m*-PA-1DA), poly(*m*-PA-2DA), and poly(BA-1DA) were 139, 169, and 157 nm, respectively (see Supporting Information, Figures S12−S14). The morphologies of dry samples of the PDA sols on mica were examined by AFM. The AFM images revealed spherical-shaped particles for poly(*m*-PA-1DA) while significant aggregation were also observed in case of poly(*m*-PA-2DA) and poly(BA-1DA). These observation supports the a relatively smaller particle size and unimodal distribution of poly(m-PA-1DA) from DLS measurement (see Supporting Information, Figure S15).

Thermochromic Properties of Polydiactylene Sols. The sols were filtered and subjected to the stepwise heating from 25 to 90 °C within a Peltier heating cell of a variable temperature UV−vis spectrometer. Figure 1 illustrates the annealing temperature dependence of the electronic absorption spectra. Upon heating, the absorption λ_{max} near 630 nm and the phonon sideband of poly(*o*-PA-1DA), poly(*m*-PA-1DA), and poly(*p*-PA-1DA) gradually shifted toward shorter wavelength. At 95 °C, the blue sols of poly(*o*-PA-1DA), poly(*m*-PA-1DA), and poly(*p*-PA-1DA) turned completely red with the absorption maximum near 540 nm, indicative of the wider band gap between the ground and excited states of the conjugated backbone. Similarly, the PDA derived from the diamidodiacetylene monomer demonstrated the same phenomena. For example, the absorption bands of poly(*m*-PA-2DA) and poly(*p*-PA-2DA) were hypsochromically shifted from λ_{max} ~640 to ~550 nm (Figure 1). The color transition temperature of the investigated PDAs, however, differed among them. The photographs of PDAs sols were recorded upon stepwise heating from 25 to 90 °C, and the results are presented in Figure 2. PDAs derived from monoamidodiacetylene, for example, poly(*o*-PA-1DA), poly(*m*-PA-1DA), and poly(*p*-PA-1DA), exhibited the blue to red color transition around 65−75 °C. The higher color transition temperatures were observed in the case of PDAs prepared from diamidodiacetylene carrying a phenylenediamine linkage such that the blue sols of poly(*m*-PA-2DA) and poly(*p*-PA-2DA) turned red around 80−90 and 70−80 °C, respectively. Substituting phenylenediamine with butanediamine or hexanediamine, the color transition temperatures were even higher. The deep blue sols of poly(BA-2DA) turned to red color around 85−95 °C while the color of poly(HA-2DA) did not appear red even at 95 °C. The other groups of PDAs, poly(*c*-CA-2DA), poly(*t*-CA-2DA), and poly(APOEO-2DA), showed relatively lower color transition temperatures around 20−25, 45−55, and 50−60 °C, respectively (Figure 2). The lower color transition temperature of poly(*t*-CA-2DA), poly(*c*-CA-2DA), and poly(APOEO-2DA) in comparison to the rest of the series confirmed the weaker

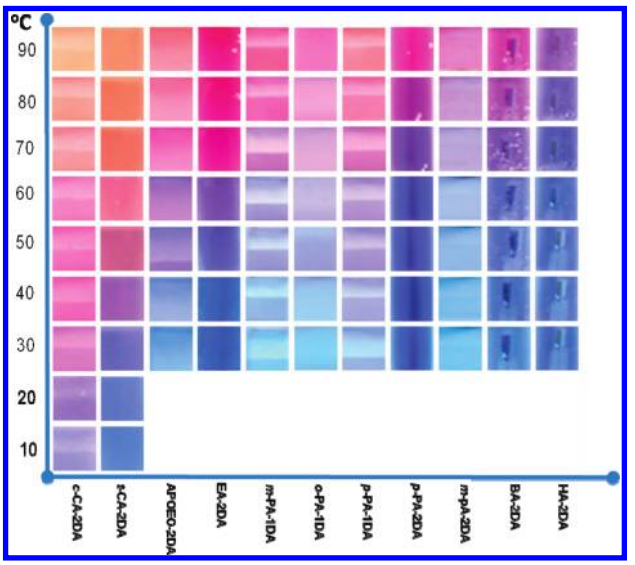

Figure 2. Color of PDA sols recorded by photography during the heating process displaying the variation of color transition temperature.

attractive interactions, viz. hydrogen bonding and hydrophobic interaction, among the side chains in these polymers. It is also interesting to note that the *trans*-geometry exhibited higher color transition temperature compared to the *cis*-geometry. The observation suggested that the diequatorial arrangement of the diamide side chains allow better packing than the axial−equatorial orientation. According to results described above, the color transition temperatures observed by eyes were in the following order: poly(HA-2DA) > poly(BA-2DA) > poly(*m*-PA-2DA) > poly(*p*-PA-2DA) > poly(*o*-PA-1DA) > poly(*m*-PA-1DA) > poly(*p*-PA-1DA) > poly(BA-2DA) > poly(APOEO-2DA) > poly(*t*-CA-2DA) > poly(*c*-CA-2DA). This order indicates the importance of the number of amide groups, the geometry of the linkers, and the lone pair electron presence in the linkers. A greater number of amide groups can lead to higher color transition temperature (poly(*m*-PA-2DA), poly(*p*-PA-2DA) > poly(*o*-PA-1DA), poly(*m*-PA-1DA), poly(*p*-PA-1DA)). The planar geometry of the linker connecting the two amides groups (poly(HA-2DA), poly(BA-2DA), poly(*m*-PA-2DA), and poly(*p*-PA-2DA)) give higher color transition temperature than those of nonplanar geometry (poly(*t*-CA-2DA) and poly(*c*-CA-2DA)). The lone electron pairs within the linker can reduce the color transition temperature (poly(APOEO-2DA) < poly(EA-2DA), poly(HA-2DA), and poly(BA-2DA)).

To quantitatively evaluate the color transition of the PDA sols, the absorbance from the electronic absorption spectra was translated into colorimetric response (%CR). The %CR is defined as percentage change in the maximum absorption of the blue phase with respect to the total absorption of both red and blue phases.[12] The plot of %CR against the temperature of all PDA studied yielded sigmoidal curves as a result of blue to red transition upon raising temperature (Figure 3). The colorimetric response plot displays a similar tendency with the photographic observation. The order of color transition temperature assessed from 40% CR is found in the following order: poly(HA-2DA) ~ poly(BA-2DA) > poly(*m*-PA-2DA) > poly(*p*-PA-2DA) > poly(*o*-PA-1DA) > poly(*m*-PA-1DA) > poly(*p*-PA-1DA) > poly(BA-2DA > poly(APOEO-2DA) > poly(*t*-CA-2DA) > poly(*c*-CA-2DA). The %CR plots also provided another piece of valuable information. Evidently, PDAs derived from *c*-CA-2DA, *t*-CA-2DA, and APOEO-2DA exhibited a rather steep sigmoid, meaning that they undergo sharp color transition within the

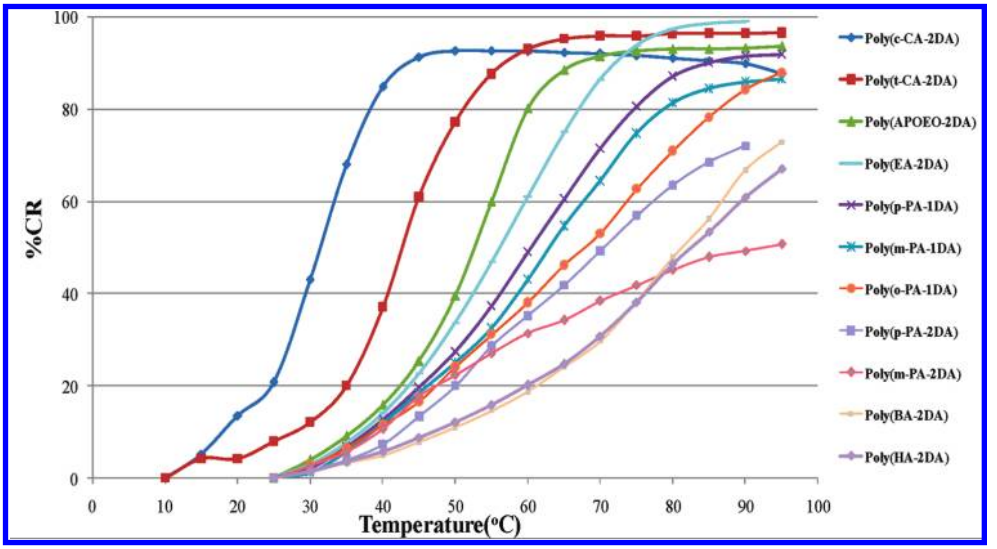

Figure 3. Colorimetric responses (%CR) of the PDA sols to the temperature upon heating.

Table 2. Thermochromic Reversibility of the PDA Sols Illustrated by Color Photographs

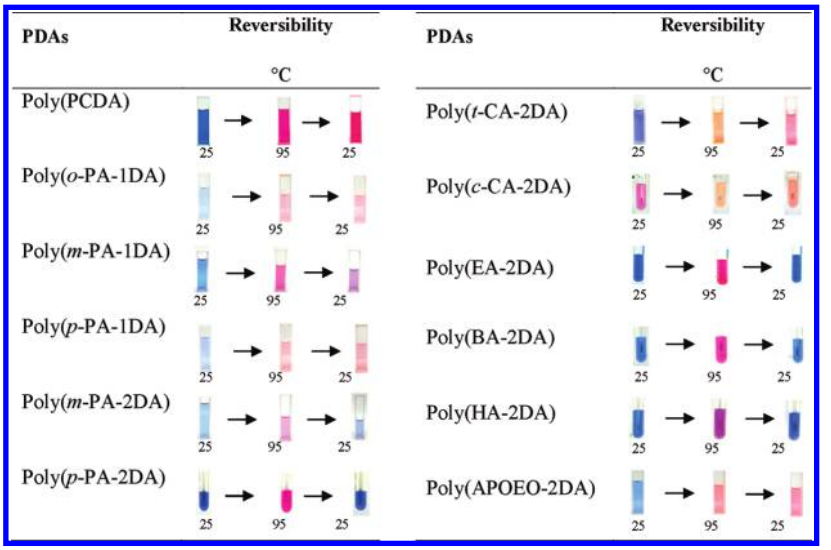

narrow ranges of temperature. The %CR of these PDAs increased from 20% to 60% within the temperature range of no more than 10 °C. On the other hand, poly(BA-2DA), poly(*o*-PA-1DA), poly(*m*-PA-1DA), and poly(*p*-PA-1DA) showed more gradual change in %CR upon heating that generally required the temperature increase of 20−25 °C to achieve the %CR transition from 20% to 60%. The PDAs derived from the monomers such as *m*-PA-2DA, *p*-PA-2DA, BA-2DA, and HA-2DA showed even slower blue to red color transition that required the increase of more than 25 °C in the temperature to attain the level of 20% to 60% CR change. The most notable trend described above is that the lower the color transition temperature, the sharper the temperature-induced colorimetric response. The intramolecular side chain interaction is again likely to be the main contribution governing this trend. The blue-to-red transition is associated with the movement of the side chains that result in the release of backbone strain or disturb the ene−yne planarity.[8] The side chain movement will be sluggish and will require more energy if the hydrophobic interaction between the side chains and the hydrogen bonding between the headgroups are strong. Since all diacetylene monomers investigated contain the same C_{25} aliphatic structure, the two hydrogen bond forming points between the headgroups are thus the main contributor to both broad temperature-induced colorimetric response and high color transition temperature. Although *c*-CA-2DA, *t*-CA-2DA, and APOEO-2DA also have two hydrogen forming points, they give PDAs with lower color transition temperature and sharper colorimetric response even when compared with the monoamide lipids like *o*-PA-1DA, *m*-PA-1DA, and *p*-PA-1DA. The results reiterate the effect of the geometry and the electron lone pair repulsion on the O atoms of the linkers between the diamide groups.

Thermochromic Reversibility of PDA Sols. During the course of the thermochromism studies, the reversibility of the color transition has come to our attention. The color of the PDA sols observed at 25 °C before heating, after heating to 95 °C, and after cooling back to 25 °C provided an approximate idea about the reversibility of these PDAs (Table 2). The PDAs possessing one amide headgroup such as poly(*o*-PA-1DA), poly(*m*-PA-1DA), and poly(*p*-PA-1DA) exhibited none to partial reversibility of the color transition while the PDAs containing diamide headgroup such as poly(*m*-PA-2DA), poly(*p*-PA-2DA), poly(EA-2DA), poly(BA-2DA), and poly(HA-2DA) displayed complete reversibility of the color transition, suggesting that the two amide headgroups are necessary for complete

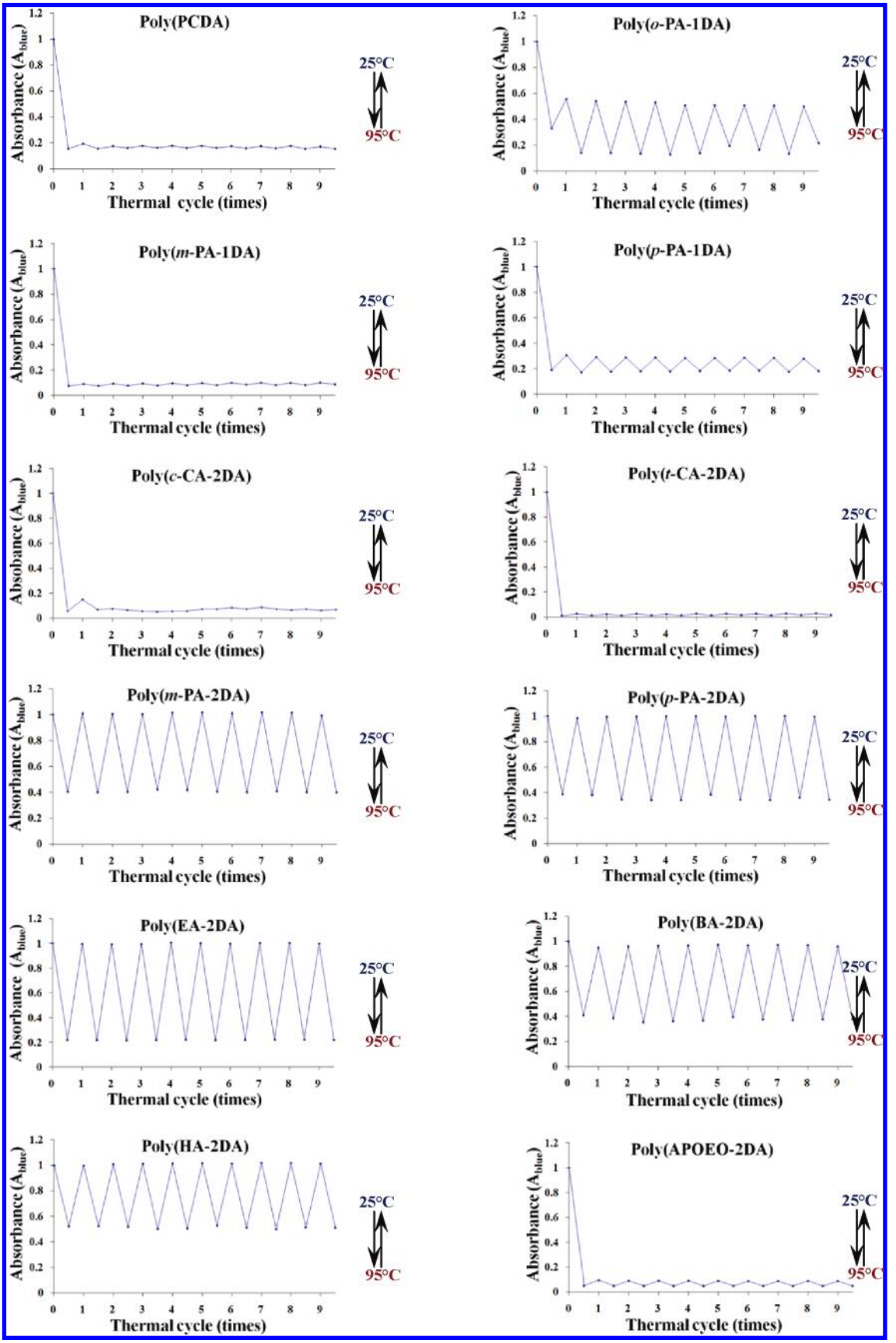

Figure 4. Absorbance at the λ_{max} of the blue sols of the PDA recoded at 25 and 95 °C in the heating−cooling cycles.

reversibility. Poly(*c*-CA-2DA), poly(*t*-CA-2DA), and poly(APOEO-2DA), however, displayed very little reversibility of the color transition despite having two amide headgroups. The results again confirm that double hydrogen bond forming among the amide headgroups in poly(*c*-CA-2DA), poly(*t*-CA-2DA), and poly(APOEO-2DA) is not geometrically feasible.

To assess the degree of thermochromic reversibility of the PDAs, the blue absorbance (A_{blue}), defined as the absorbance at the λ_{max} of the "blue phase", was monitored for nine cycles of heating and cooling between 95 and 25 °C. The plots between the absorbance and the cycle numbers of poly(*m*-PA-2DA), poly(*p*-PA-2DA), poly(EA-2DA), poly(BA-2DA), and poly(HA-2DA) displayed a zigzag pattern with virtually full recovery of the initial absorbance in every cycles (Figure 4), indicating the complete thermochromic reversibility of these PDAs. Again, two points of hydrogen bond forming between the diamide headgroups probably play the crucial roles in this reversibility. The rest of the PDAs did not show full reversibility as the blue absorbance dropped dramatically after the first heating−cooling cycle. Interestingly, all of these PDAs, except poly(*c*-CA-2DA), however, showed certain degrees of consistent reversibility from the second heating−cooling cycle. The abilities to regain the intensity of the initial blue absorbance are diverse among them. For comparison, thermochromic reversibility of poly(PCDA) was studied in the same manner. Poly(PCDA) showed a low degree but consistent recovery of the blue phase absorbance after the second heating−cooling cycle. The recoveries of the blue absorbance of the monoamide PDAs whose side chains contain aromatic rings, such as poly(*o*-PA-1DA) and poly(*p*-PA-1DA), were notably greater than that of poly(PCDA). The results signify the contribution of the $\pi-\pi$ interaction between the aromatic rings to the reversibility of the color transition.

To obtain a quantitative value of the degree of reversibility (%DR), the average value of the absorbance change (ΔA_{avg}) from the second to ninth heating is compared against the absorbance change in the first heating (ΔA_1) according to the following equation: $\%DR = 100 \times \Delta A_{avg}/\Delta A_1$ where $\Delta A = A_{25\,°C} - A_{95\,°C}$. On the basis of %DR presented in Table 3, three reversibility classes of the PDAs, i.e., fully reversible PDA (%DR ≥ 90%), partially reversible PDA (10 < %DR < 90%), and irreversible PDA (%DR ≤ 10%), can be perceived. Using the classification mentioned above, poly(*m*-PA-1DA), poly(*t*-CA-2DA), poly(*c*-CA-2DA), poly(APOEO-2DA), and poly(PCDA) possess irreversible thermochromic property. After the second heating−cooling cycle, these polymers appeared as red color at both 95 and 25 °C (Table 3). The small recovery (1−5%) observed in these PDAs is conceivably the result of either the difference in the side chain packing or the altering of the vibronic state population at different temperatures.

In consideration of thermodynamic reversibility of the color transition of PDAs, the enthalpy change (ΔH) is likely to be the major contributor to the free energy change ($\Delta G = \Delta H - T\Delta S$) as the entropic term ($T\Delta S$) is insignificant in condensed matter such as vesicles. Providing that the thermochromic process is a unimolecular process excluding solvent interference, the enthalpy term (ΔH) can be thought as a sum of several bonding and steric energy terms, i.e., hydrogen bonding between the headgroups (ΔH_{hb}), hydrophobic interaction among the side chains (ΔH_{hi}), conformational strain of individual side chain (ΔH_{cs}), backbone strain (ΔH_{bs}), and delocalization energy within the conjugated system (ΔH_{de}). Thus, $\Delta H = \Delta H_{hb} + \Delta H_{hi} + \Delta H_{cs} + \Delta H_{bs} + \Delta H_{de}$. Upon heating, ΔH_{hb}, ΔH_{hi}, and ΔH_{de} are positive while ΔH_{bs} is negative because the hydrogen bonding, hydrophobic interaction, delocalization energy, and backbone strain are present in the original blue form to a greater extent compared to the red form. Earlier literature works have reported that the side chains in the blue form contain more gauche conformation than those in the red form,[13] suggesting that ΔH_{cs} is negative upon heating. In the irreversible process, the positive enthalpy changes (ΔH_{hb}, ΔH_{hi}, and ΔH_{de}) are either less than or comparable to the negative enthalpy changes (ΔH_{cs} and ΔH_{bs}). In the other words, the thermodynamic stability gained from the hydrogen bonding, hydrophobic interaction, and delocalization energy in the blue form are not enough to restore the original conformation and backbone strains. The partially reversible thermochromism observed for poly(*o*-PA-1DA) and poly(*p*-PA-1DA) indicates that the red form is a metastable form present only at high temperature, where the entropic term ($T\Delta S$) becomes significant, while the purple color is the stable phase that exists after the PDAs are cooled back to room temperature (see Table 2 for the appearing color). This stable purple color obtained is different from the purple form observed at intermediate temperature (~50−60 °C) during the first heating which is only metastable akin to the metastable purple form of poly(PCDA).[10c] In these polymers, the extra benzene rings add hydrophobic and $\pi-\pi$ interaction to help in restoring some of the original conformation and backbone strains. The complete reversibility observed for poly(*m*-PA-2DA), poly(*p*-PA-2DA), poly(BA-2DA), and poly(HA-2DA) is for the most part attributed to the dual hydrogen bond forming between the diamide headgroups. It is likely that at least one of the hydrogen bonds per headgroup remained strongly present up to 95 °C. The red form of theses PDAs is a metastable form which is present only at high temperature where the entropic term becomes more influential.

Table 3. Degree of Reversibility and the Classification of the PDA Sols Determined from the Absorption Spectra in Figure 4

PDA	degree of reversibility (%)	classification of PDA
poly(PCDA)	2.2	irreversible
poly(*m*-PA-1DA)	1.7	irreversible
poly(*c*-CA-2DA)	1.2	irreversible
poly(*t*-CA-2DA)	1.2	irreversible
poly(APOEO-2DA)	4.3	irreversible
poly(*o*-PA-1DA)	55	partially reversible
poly(*p*-PA-1DA)	13	partially reversible
poly(*m*-PA-2DA)	101	fully reversible
poly(*p*-PA-2DA)	105	fully reversible
poly(EA-2DA)	100	fully reversible
poly(BA-2DA)	100	fully reversible
poly(HA-2DA)	105	fully reversible

Conclusion

The color transition temperature and thermochromic reversibility of polydiacetylenes can be tuned by the variation of the number of internal amide functional groups in the monomers and the structures of the linkers between the amide groups. Both color transition temperature and reversibility of polydiacteylenes were found to be mainly associated with the number and orientation of the hydrogen bond forming groups. The sensibility and degree of colorimetric reversibility, which are extremely important factors for development of materials for temperature indicators, can be assessed via the determination of the colorimetric response (%CR) and the degree of reversibility (%DR), respectively. The capability of tuning the color transition temperature as well as the reversibility of the color transition will surely expand the scope where polydiacetylenes can be applied.

Experimental Section

Chemicals and Instrumentation. 10,12-Pentacosanoic acid (PCDA) was purchased from GFS Chemical, and other reagents were purchased from Sigma-Aldrich and Fluka. Analytical grade solvents such as chloroform and methylene chloride were used without further purification. Flash chromatography was

carried out on silica gel 60 (230−400 mesh; Merck). Thin layer chromatography (TLC) was carried out using Merck 60 F_{254} plates with a thickness of 0.25 mm. The diacetylene monomers were purified by filtration to remove the polymerized lipid before used. The ^{1}H and ^{13}C NMR spectra were collected on a 400 MHz NMR spectrometer (Murcury 400, Varian). The molecular weights were obtained from a low-resolution quadupole mass analyzer (Quattro Micro API 2000, Micromass) using the electrospraying ionization (ESI) technique. The electronic absorption spectra were recorded on a temperature variable UV−vis spectrophotometer (Carry 100Bio, Varian).The AFM images were acquired with Nano Scope IV (Vecco Metrology Group) operating by noncontact mode. The particle size measurements were made by a dynamic light scattering using a nanosizer (Malvern Instruments).

General Procedure for Synthesis of Monoamidodiacetylene Lipid Monomers. 1-Ethyl-3-(3′-dimethylamino)carbodiimide HCl salt (EDCI) (230.04 mg, 1.2 mmol) in chloroform (4 mL) was added dropwise into a solution of 10,12-pentacosadiynoic acid (374.61 mg, 1.0 mmol) in chloroform (5 mL). The mixture was stirred for 1 h at 0 °C and was then added dropwise into 1.5 equiv of the selected diamine, e.g., 1,2-phenylenediamine (162.21 mg, 1.5 mmol) in chloroform (4 mL) at 0 °C. The reaction mixture was stirred at room temperature overnight when the white precipitate was clearly observed. The reaction mixture was evaporated under reduced pressure to yield the crude product as a white solid. Purification was accomplished by column chromatography on silica gel eluted with a mixture of hexane and ethyl acetate (50:50) to give *o*-PA-1DA (386 mg, 47%) as a white solid; mp 82−84 °C. ^{1}H NMR (400 MHz, $CDCl_3$): δ 9.07 (1H, s, NHC═O), 7.11 (1H, d, J = 7.5 Hz, ArH), 6.86 (1H, t, J = 7.5 Hz, ArH), 6.68 (1H, d, J = 7.5 Hz, ArH), 6.51 (1H, t, J = 7.5 Hz, ArH), 4.78 (2H, br, NH_2), 2.41−2.06 (6H, m, $3CH_2$), 1.65−1.03 (32H, m, $16CH_2$), 0.83 (3H, t, J = 6.5 Hz, CH_3). LRMS calcd for $C_{31}H_{48}N_2ONa$ $[M + Na]^+$: 488.7; found: 487.7. *m*-PA-1DA (427 mg, 52%); mp 76−78 °C. ^{1}H NMR (400 MHz, $CDCl_3$): δ 9.51 (1H, s, NHC═O), 6.88 (1H, s, ArH), 6.64 (1H, d, J = 8.5 Hz, 2ArH), 6.21 (1H, d, J = 8.0 Hz, ArH), 5.00 (2 H, s, NH_2), 2.24 (6 H, m, $3CH_2$), 1.65−1.15 (32H, m, $16CH_2$), 0.84 (3H, t, J = 7.0 Hz, CH_3). LMRS calcd for $C_{31}H_{49}N_2O$ $[M + H]^+$: 465.38; found: 465.47. *p*-PA-1DA (452 mg, 55%); mp 101−103 °C. ^{1}H NMR (400 MHz, $CDCl_3$): δ 9.42 (1H, s, NH═CO), 7.19 (2H, d, J = 8.5 Hz, 2ArH), 6.48 (2H, d, J = 8.5 Hz, 2ArH), 4.98−4.77 (2H, m, NH_2), 2.23 (6H, td, J = 15.0, 7.0 Hz, $3CH_2$), 1.65−1.04 (32H, m, $16CH_2$), 0.85 (3H, t, J = 6.5 Hz, CH_3). LMRS calcd for $C_{31}H_{48}N_2ONa$ $[M + Na]^+$: 488.73; found: 487.37.

General Procedure for Synthesis of Diamidodiacetylene Lipid Monomers. 1-Ethyl-3-(3′-dimethylamino)carbodiimide HCl salt (EDCI) (383.4 mg, 2 mmol) in chloroform (2 mL) was added dropwise into a solution of 10,12-pentacosadiynoic acid (637 mg, 1.7 mmol) in chloroform (2 mL). After stirring for an hour, 0.45 equiv of the selected diamine, e.g., 1,2-phenylenediamine (81 mg, 0.75 mmol) in chloroform (10 mL), was then added dropwise and kept stirred overnight. The reaction mixture was evaporated under reduced pressure to yield the crude product as a white solid. The crude product was then crystallized in methanol to afford ***o*-AP-2DA** (370 mg, 60%); mp 112−114 °C. ^{1}H NMR (400 MHz, $CDCl_3$): δ = 8.05−7.98 (2H, br, NH═CO), 7.42−7.36 (2H, m, 2ArH), 7.22−7.17 (2H, m, 2ArH), 2.36 (4H, t, J = 7.5 Hz, $2CH_2$), 2.24 (8H, dd, J = 9.0, 4.52 Hz, $4CH_2$), 1.78−1.18 (64H, m, $32CH_2$), 0.88 (6H, t, J = 7.0 Hz, $2CH_3$). LMRS calcd for $C_{56}H_{88}N_2O_2Na$ $[M + Na]^+$: 844.68; found: 843.74. ***m*-PA-2DA** (320 mg, 52%); mp 103−105 °C. ^{1}H NMR (400 MHz, $CDCl_3$): δ = 7.86−7.79 (2H, br, NH═CO), 7.30−7.24 (2H, m, 2ArH), 7.18−7.16 (2H, m, 2ArH), 2.33 (4H, t, J = 7.5 Hz, $2CH_2$), 2.24 (8H, t, J = 6.5 Hz, $4CH_2$), 1.76−1.18 (64H, m, $32CH_2$), 0.88 (6H, t, J = 6.5 Hz, $2CH_3$). LMRS calcd for $C_{56}H_{88}N_2O_2Na$ $[M + Na]^+$: 844.68; found: 844.16. ***p*-PA-2DA** (363 mg, 59%); mp 167−169 °C. ^{1}H NMR (400 MHz, $CDCl_3$): δ = 7.47 (4 H, s, 4ArH), 7.07 (2H, br, NH═CO), 2.33 (4H, t, J = 7.0 Hz, $2CH_2$), 2.24 (8H, t, J = 7.0 Hz, $2CH_2$), 1.78−1.18 (64H, m, $32CH_2$), 0.88 (6H, t, J = 7.0 Hz, $2CH_3$). LMRS calcd for $C_{56}H_{87}N_2O_2$ $[M - H]^-$: 819.68; found: 819.83. ***c*-CA-2DA** (323 mg, 52%); mp 62−64 °C. ^{1}H NMR (400 MHz, $CDCl_3$): δ = 6.28 (2H, br, NH═CO), 3.95−4.00 (2H, m, 2CH), 2.21 (12H, td, J = 15.0, 7.0 Hz, $6CH_2$), 1.89 (4H, d, J = 1.5 Hz, $2CH_2$), 1.70−1.13 (68 H, m, $34CH_2$), 0.88 (6H, t, J = 6.5 Hz, $2CH_3$). LMRS calcd for $C_{56}H_{94}N_2O_2Na$ $[M + Na]^+$: 849.73; found: 850.27. *t*-CA-2DA (379 mg, 61%); mp 62−64 °C. ^{1}H NMR (400 MHz, $CDCl_3$): δ = 5.87 (2H, br, NH═CO), 3.74−3.56 (2H, m, 2CH), 2.49−1.97 (16H, m, $8CH_2$), 1.82−1.15 (68H, m, $34CH_2$), 0.88 (6H, t, J = 6.5 Hz, $2CH_3$). **EA-2DA** (197.9 mg, 52%); mp 125−130 °C. ^{1}H NMR (400 MHz, $CDCl_3$): δ = 6.10 (2H, br, NH═CO), 3.39 (4H, br, $2CH_2$), 2.17 (8H, t, J = 7.0 Hz, $4CH_2$), 2.10 (4H, t, J = 7.5 Hz, $2CH_2$), 1.25−1.51 (64H, m, $32CH_2$), 0.88 (6H, t, J = 6.8 Hz, $2CH_3$). **BA-2DA** (451 mg, 75%); mp 117−120 °C. ^{1}H NMR (400 MHz, $CDCl_3$): δ = 6.34 (2H, br, NH═CO), 3.28 (4H, m, $2CH_2$), 2.22 (12H, t, J = 7.0 Hz, $6CH_2$), 1.68−1.15 (66H, m, $33CH_2$), 0.86 (6H, t, J = 6.5 Hz, $2CH_3$). LMRS calcd for $C_{37}H_{75}N_2O_2$ $[M - C_{17}H_{27}]^+$: 570.51; found: 569.72. **HA-2DA** (404 mg, 65%); mp 122−125 °C. ^{1}H NMR (400 MHz, $CDCl_3$): δ = 5.56 (2H, br, NH═CO), 3.24 (4H, q, J = 6.5 Hz, $2CH_2$), 2.20 (12H, td, J = 15.0, 7.5 Hz, $6CH_2$), 1.71−1.13 (72H, m, $36CH_2$), 0.88 (6H, t, J = 6.5 Hz, $2CH_3$). LMRS calcd for $C_{56}H_{96}N_2O_2Na$ $[M + Na]^+$: 852.75; found: 850.27. **APOEO-2DA** (504 mg, 72%); mp 77−80 °C. ^{1}H NMR (400 MHz, $CDCl_3$): δ = 6.17 (2H, br, NH═CO), 3.71−3.49 (16H, m, $8CH_2$), 3.35 (4H, q, J = 6.0 Hz, $2CH_2$), 2.18 (12H, td, J = 15.0, 7.5 Hz, $6CH_2$), 1.83−1.17 (64H, m, $32CH_2$), 0.87 (6H, t, J = 6.5 Hz, $2CH_3$).

Typical Method for Preparation of Polydiacetylene Vesicles. A diacetylene monomer was dissolved in chloroform (0.5 mL) in a test tube, and the solvent was removed under reduced pressure. A volume of Milli-Q water was added to provide the lipid concentration of 0.25 mM. The suspension was heated to 75−85 °C and sonicated in an ultrasonicating bath until a translucent vesicle sol was obtained, typically requiring 30−40 min. The vesicle sol was kept at 4 °C overnight and was then irradiated with UV lamp (254 nm, 500 μW/cm^2) for 5 min at room temperature, unless specified otherwise, and filtered through a filter paper (No. 1) to give a clear intense blue vesicle sol. The PDA sols were characterized by UV−vis absorption, dynamic light scattering, and AFM imaging as described in the Results and Discussion. Freeze-dried samples of some PDAs were also characterized by Raman spectroscopy for the presence of the ene−yne conjugate. Raman peaks (cm^{-1}) for poly(*m*-PA-2DA): 1510 (C═C), 2112 (C≡C); poly(*p*-PA-2DA): 1515 (C═C), 2104 (C≡C); poly(BA-2DA): 1506 (C═C), 2107 (C≡C); poly(HA-2DA): 1514 (C═C), 2115 (C≡C).

Acknowledgment. This study was financially supported by the grants from National Nanotechnology Center, National Science and Technology Development Agency (NANOTEC, NSTDA), and the Thailand Research Fund (DIG 5180020). We also thank Center for Petroleum, Petrochemicals and Advanced Materials, Chulalongkorn University and the 90th Anniversary of Chulalongkorn University Fund (Ratchadaphiseksomphot Endowment Fund) for student scholarships.

Supporting Information Available: ^{1}H NMR spectra of all monomers, atomic force microscopic images, dynamic light scattering plots, and Raman spectra. This material is available free of charge via the Internet at http://pubs.acs.org.

References and Notes

(1) (a) Baughman, R. H. *J. Appl. Phys.* **1972**, *43*, 4362–4370. (b) Sandstedt, C. A.; Eckardt, C. J.; Downey, M. J.; Sandman, D. J. *Chem. Mater.* **1994**, *6*, 1346–1350.

(2) (a) Day, D.; Ringsdorf, H. *J. Polym. Sci., Polym. Lett*. **1978**, *16*, 205–210. (b) Charych, D.; Nagy, J. O.; Spevak, M. D.; Bednarski, M. D. *Science* **1993**, *261*, 585–588. (c) Batchelder, D. N.; Evans, S. D.; Freeman, T. I.; Haussling, L. *J. Am. Chem. Soc*. **1994**, *116*, 1050–1053. (d) Kuriyama, K.; Kikuchi, H.; Kajiyama, T. *Langmuir* **1998**, *14*, 1130–1138. (e) Huang, X.; Jiang, S.; Liu, M. *J. Phys. Chem. B* **2005**, *109*, 114–119.

(3) (a) Reichert, A.; Nagy, J. O.; Spevak, W.; Charych, D. *J. Am. Chem. Soc*. **1995**, *117*, 829–830. (b) Cheng, Q.; Yamamoto, M.; Stevens, R. C. *Langmuir* **2000**, *16*, 5333–5342. (c) Song, J.; Cheng, Q.; Kopta, S.; Stevens, R. C. *J. Am. Chem. Soc*. **2001**, *123*, 3205–3213. (d) Lu, Y.; Yang, Y.; Lu, M.; Huang, J.; Fan, H.; Haddad, R.; Burns, A. R.; Saaki, D. Y.; Shelnutt, J.; Sellinger, A.; Lopez, G.; Brinker, C. J. *Nature* **2001**, *410*, 913–917. (e) Yang, Y.; Lu, Y.; Lu, M.; Huang, J.; Haddad, R.; Xomeritakis, G.; Liu, N.; Malanoski, A. P.; Sturmavr, D.; Fan, H.; Sasaki, D. Y.; Assink, R. A.; Shelnutt, J. A.; Swol, F. V.; Lopez, G. P.; Burns, A. R.; Brinker, C. J. *J. Am. Chem. Soc*. **2003**, *25*, 1269–1277. (f) Song, J.; Cisar, J. S.; Bertozzi, C. R. *J. Am. Chem. Soc*. **2004**, *126*, 8459–8465. (g) Lee, S. B.; Koepsel, R. R.; Russell, A. J. *Nano Lett*. **2005**, *5*, 2202–2206. (h) Dautel, O. J.; Robitzer, M.; LePorte, J. P.; Serein-Spirau, F.; Moreau, J. I. *J. Am. Chem. Soc*. **2006**, *128*, 16213–16223. (i) Simon, J. K.; Elizabeth, A. H. *J. Mater. Chem*. **2006**, *16*, 2039–2047.

(4) (a) Cheng, Q.; Stevens, R. C. *Langmuir* **1998**, *14*, 1974–1976. (b) Kolusheva, S.; Shahal, T.; Jelinek, R. *J. Am. Chem. Soc*. **2000**, *122*, 776–780. (c) Kim, J. M.; Ji, E. K.; Woo, S. M.; Lee, H. W.; Ahn, D. J. *Adv. Mater*. **2003**, *15*, 1118–1121. (d) Kew, S. J.; Hall, E. A. *Anal. Chem*. **2006**, *78*, 2231–2238. (e) Potisatityuenyong, A.; Tumcharern, G.; Dubas, S. T.; Sukwattanasinitt, M. *J. Colloid Interface Sci*. **2006**, *304*, 45–51. (f) Yoon, J.; Jung, Y. S.; Kim, J. M. *Adv. Funct. Mater*. **2009**, *19*, 209–214. (g) Champaiboon, T.; Tumcharern, G.; Potisatityuenyong, A.; Wacharasindhu, S.; Sukwattanasinitt, M. *Sens. Actuators, B* **2009**, *139*, 532–537. (h) Chen, X.; Lee, J.; Jou, M. J.; Kim, J.-M.; Yoon, J. *Chem. Commun*. **2009**, 3434–3436.

(5) (a) Charych, D.; Cheng, Q.; Reichert, A.; Kuziemko, G.; Stroh, M.; Nagy, J. O.; Spevak, W.; Stevens, R. C. *Chem. Biol*. **1996**, *3*, 113–120. (b) Cheng, Q.; Stevens, R. C. *Adv. Mater*. **1997**, *9*, 481–483. (c) Okada, S. Y.; Jelinek, R.; Charych, D. *Angew. Chem., Int. Ed*. **1999**, *38*, 655–659. (d) Kolusheva, S.; Boyer, L.; Jelinek, R. *Nat. Biotechnol*. **2000**, *18*, 225–227. (e) Kolusheva, S.; Kafri, R.; Katz, M.; Jelinek, R. *J. Am. Chem. Soc*. **2001**, *123*, 417–422. (f) Gill, I.; Ballesteros, A. *Angew. Chem., Int. Ed*. **2003**, *42*, 3264–3267. (g) Rangin, M.; Basu, A. *J. Am. Chem. Soc*. **2004**, *126*, 5038–5039. (h) Ma, G. Y.; Cheng, Q. *Langmuir* **2005**, *21*, 6123–6126. (i) Su, Y.; Li, J.; Jiang, L.; Cao, J. *J. Colloid Interface Sci*. **2005**, *284*, 114–119. (j) Jung, Y. K.; Park, H. G.; Kim, J. M. *Biosens. Bioelectron*. **2006**, *21*, 1536–1544. (k) Wang, C.; Mar, Z.; Su, Z. *Sens. Actuators, B* **2006**, *113*, 510–515. (l) Reppy, M. A.; Pindzola, B. A. *Chem. Commun*. **2007**, *42*, 4317–4338. (m) Deng, J. L.; Sheng, Z. H.; Zhou, K.; Duan, M. X.; Yu, C. Y.; Jiang, L. *Bioconjugate Chem*. **2009**, *20*, 533–537.

(6) Mino, N.; Tamura, H.; Ogawa, K. *Langmuir* **1992**, *8*, 594–598.

(7) (a) Exarhos, G. J.; Risen, W. M.; Baughman, R. H. *J. Am. Chem. Soc*. **1976**, *98* (2), 481–487. (b) Chance, R. R.; Baughman, R. H.; Mueller, H.; Eckhardt, C. J. *J. Chem. Phys*. **1977**, *67*, 3616–3618.

(8) (a) Chance, R. R. *Macromolecules* **1980**, *13*, 396–398. (b) Rubner, M. F.; Sandman, D. J.; Velazquez, C. *Macromolecules* **1987**, *20*, 1296–1300. (c) Beckham, H. W.; Rubner, M. F. *Macromolecules* **1993**, *26*, 5198–5201. (d) Deckert, A. A.; Horne, J. C.; Valentine, B.; Kiernan, L.; Fallon, L. *Langmuir* **1995**, *11*, 643–649. (e) Hammond, P. T.; Rubner, M. F. *Macromolecules* **1997**, *30*, 5773–5782. (f) Lio, A.; Reichert, A.; Ahn, D. J.; Nagy, J. O.; Salmeron, M.; Charych, D. H. *Langmuir* **1997**, *13*, 6524–6532. Carpick, R. W.; Mayer, T. M.; Sasaki, D. Y.; Burns, A. R. *Langmuir* **2000**, *16*, 4639–4647. (g) Lee, D. C.; Sahoo, S. K.; Cholli, A. L.; Sandman, D. J. *Macromolecules* **2002**, *35*, 4347–4355. (h) Wang, X.; Whitten, J. E.; Sandman, D. J. *J. Chem. Phys*. **2007**, *126*, 184905.

(9) (a) Okada, S.; Peng, S.; Spevak, W.; Charych, D. *Acc. Chem. Res*. **1998**, *31*, 229–239. (b) Itoh, T.; Shichi, T.; Yui, T.; Takahashi, H.; Inui, Y.; Yakagi, K. *J. Phys. Chem. B* **2005**, *109*, 3199–3206.

(10) (a) Huo, Q.; Russell, K. C.; Leblanc, R. M. *Langmuir* **1999**, *15*, 3972–3980. (b) Kim, J. M.; Lee, J. S.; Choi, H.; Sohn, D.; Ahn, D. J. *Macromolecules* **2005**, *38*, 9366–9376. (c) Yuan, Z. Z.; Lee, C. W.; Lee, S. H. *Polymer* **2006**, *47*, 2970–2975. (d) Potisatityuenyong, A.; Rojanathanes, R.; Tumcharern, G.; Sukwattanasinitt, M. *Langmuir* **2008**, *24*, 4461–4463.

(11) Wang, X.; Sandman, D. J.; Chen, S.; Gido, S. P. *Macromolecules* **2008**, *41*, 773–778.

(12) Reichert, A.; Nagy, J. O.; Spevak, W.; Charych, D. H. *J. Am. Chem. Soc*. **1995**, *117*, 829–830.

(13) (a) Dobrosavljevic, V.; Stratt, R. M. *Phys. Rev. B* **1987**, *35*, 2781–2794. (b) Schott, M. *J. Phys. Chem. B* **2006**, *110*, 15864–15868.